Nonequilibrium thermodynamics and power generation in open quantum optomechanical systems

Paulo J. Paulino [1,*] Igor Lesanovsky [1,2] and Federico Carollo [1]

[1] *Institut für Theoretische Physik, Eberhard Karls Universität Tübingen, Auf der Morgenstelle 14, 72076 Tübingen, Germany*

[2] *School of Physics and Astronomy and Centre for the Mathematics and Theoretical Physics of Quantum Non-Equilibrium Systems, University of Nottingham, Nottingham NG7 2RD, United Kingdom*

Cavity optomechanical systems are a paradigmatic setting for the conversion of electromagnetic energy into mechanical work. Experiments with atoms coupled to cavity modes are realized in nonequilibrium conditions, described by phenomenological models encoding nonthermal dissipative dynamics and falling outside the framework of weak system-bath couplings. This fact makes their interpretation as quantum engines, e.g., the derivation of a well-defined efficiency, quite challenging. Here, we present a consistent thermodynamic description of open quantum cavity-atom systems. Our approach takes advantage of their nonequilibrium nature and arrives at an energetic balance which is fully interpretable in terms of persistent dissipated heat currents. The interaction between atoms and cavity modes can further give rise to nonequilibrium phase transitions and emergent behavior and allows us to assess the impact of collective many-body phenomena on the engine operation. To enable this, we define two thermodynamic limits, one related to a weak optomechanical coupling and one related to a strong optomechanical coupling. We illustrate our ideas by focusing on a time-crystal engine and discuss power generation, energy-conversion efficiency, and the emergence of metastable behavior in these limits.

I. INTRODUCTION

The application of thermodynamics to quantum systems [1–6] allows us to conceive quantum heat engines, which perform ideal cycles between thermal equilibrium states [7–9]. In many experiments of interest, however, quantum systems are realized under genuine out-of-equilibrium conditions, for example, in the case of experiments with cold atoms in optomechanical cavities [10–20] [see the sketch in Fig. 1(a)]. These systems absorb energy from an external source, e.g., a laser, which prevents them from equilibrating with their surrounding and gives rise to persistent energy currents. This aspect motivates the development of alternative nonequilibrium quantum-engine cycles [21,22], with driving protocols that are not described by thermal dynamics [23,24]. It further poses the problem of devising theoretical approaches [25–32] providing a *consistent* thermodynamic understanding of established experimental models [19,33–35]. These open challenges do not solely concern quantum systems and are of much broader relevance, as indicated by recent efforts to characterize work in active matter [36–43].

In this paper, we focus on paradigmatic open quantum optomechanical systems which can nowadays be realized and efficiently controlled in experiments [10–19,44–48]. These setups are promising for the conversion of electromagnetic energy into mechanical work in both equilibrium [49,50] and nonequilibrium conditions [51–54]. For these systems,

we develop a thermodynamic description which characterizes the power transferred by the cavity to the mechanical oscillator [see Fig. 1(b)] as well as the efficiency of this energy conversion. Our approach allows us to formulate an energy balance in terms of the persistent nonequilibrium heat currents [see Fig. 1(b)]. To investigate the impact of phase transitions and collective behavior on the performance of nonequilibrium engines, we consider two different thermodynamic limits [55–60] [see Fig. 1(c)]. One features a weak optomechanical coupling, ensuing from a finite density of atoms in the cavity [59], and is characterized by finite power and zero efficiency. The other one features a strong optomechanical coupling due to an infinite density of atoms. In this case, the delivered mechanical power is extensive in the "size" of the system and the efficiency is finite.

We illustrate our ideas by exploiting a time-crystal [61–65] engine, which is a manifestation of a nonequilibrium many-body quantum engine [59,66,67]. Our results also apply to generic optomechanical settings [19,46] and related spin-boson models, such as Rydberg-atom systems with interacting electronic and vibrational degrees of freedom [68,69] and superconducting-qubit systems [70].

II. THE MODEL

We consider the setup in Fig. 1(a), which shows an ensemble of N atoms loaded into a cavity. The atoms are described by two-level systems with ground state $|g\rangle$, excited state $|e\rangle$, and bare Hamiltonian $H_{\mathrm{at}} = \hbar\omega_{\mathrm{at}} \sum_{k=1}^{N} n^{(k)}$, where $n = |e\rangle\langle e|$. The bare-cavity Hamiltonian is $H_{\mathrm{cav}} = \hbar\omega_{\mathrm{cav}} a^\dagger a$, with a and $a^\dagger$ being the cavity-mode operators. The atoms and the cavity
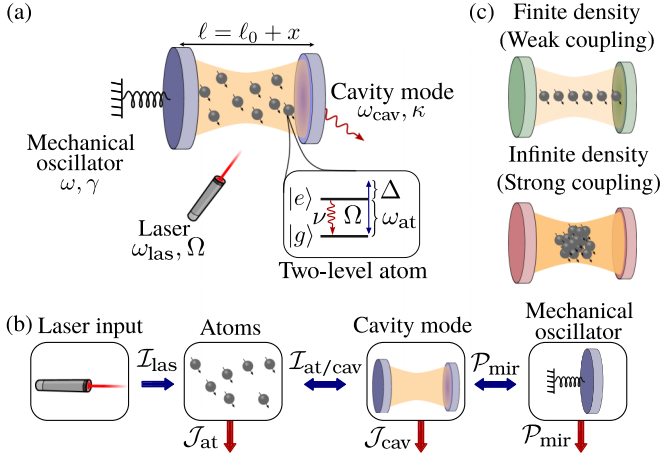
---

*paulo.paulino.souza96@gmail.com

FIG. 1. Nonequilibrium cavity-atom optomechanical engine. (a) Atoms in a cavity are driven by a laser with Rabi frequency Ω and detuning Δ. One of the cavity mirrors can move, allowing for oscillations of the cavity length ℓ from its equilibrium position ℓ_0. (b) The laser provides energy which flows through the cavity to the mirror. Atom and photon losses at rates ν and κ, respectively, determine energy dissipation. The mechanical power delivered by the engine equals the power the mirror dissipates due to friction. (c) Two possible thermodynamic limits for the system. The first features a finite density of atoms and results in a weak optomechanical coupling. The second features an infinite density of atoms, giving rise to a strong optomechanical coupling.

mode interact through a Tavis-Cummings term [71–73],

$$H_{\text{int}} = \frac{\hbar g}{\sqrt{N}}(aS_+ + a^\dagger S_-), \tag{1}$$

where $S_- = \sum_{k=1}^{N} \sigma_-^{(k)}$, with $\sigma_- = |g\rangle\langle e|$, and $S_+ = S_-^\dagger$. The atoms are further driven by a laser which, in combination with the bare-atom energy, is described by the Hamiltonian (in the interaction picture)

$$H_{\text{las}} = \hbar\Omega(S_- + S_+) - \hbar\Delta \sum_{k=1}^{N} n^{(k)}, \tag{2}$$

where Ω is the Rabi frequency and $\Delta = \omega_{\text{las}} - \omega_{\text{at}}$ is the detuning of the laser frequency from the atom transition frequency [see Fig. 1(a)].

The dynamics of the system state ρ_t is governed by the master equation [74] (in the interaction picture)

$$\dot\rho_t = \mathcal{L}[\rho_t] := -\frac{i}{\hbar}[H, \rho_t] + \mathcal{D}_{\text{at}}[\rho_t] + \mathcal{D}_{\text{cav}}[\rho_t], \tag{3}$$

with Hamiltonian $H = H_{\text{las}} + H_{\text{int}} - \hbar\delta a^\dagger a$ and $\delta = \omega_{\text{las}} - \omega_{\text{cav}}$. The dissipators $\mathcal{D}_{\text{at/cav}}$ account for irreversible effects due to a coupling of the atoms and the light field to thermal reservoirs at inverse temperature β. For the atoms, we have the dissipator

$$\mathcal{D}_{\text{at}}[\rho] = \nu \sum_{k=1}^{N} \left(\sigma_-^{(k)} \rho \sigma_+^{(k)} - \frac{1}{2}\{n^{(k)}, \rho\}\right)$$

$$+ \nu e^{-\beta\hbar\omega_{\text{at}}} \sum_{k=1}^{N} \left(\sigma_+^{(k)} \rho \sigma_-^{(k)} - \frac{1}{2}\{1 - n^{(k)}, \rho\}\right),$$

while for the light field the dissipator reads

$$\mathcal{D}_{\text{cav}}[\rho] = \kappa \left(a\rho a^\dagger - \frac{1}{2}\{a^\dagger a, \rho\}\right)$$

$$+ \kappa e^{-\beta\hbar\omega_{\text{cav}}} \left(a^\dagger \rho a - \frac{1}{2}\{aa^\dagger, \rho\}\right).$$

Both encode the spontaneous atom (photon) decay at rate ν (κ) and atom (photon) excitation at rate $\nu e^{-\beta\omega_{\text{at}}}$ ($\kappa e^{-\beta\omega_{\text{cav}}}$). The latter excitation process is often irrelevant in experiments since $\beta\hbar\omega_{\text{cav/at}} \gg 1$ [19].

The cavity further features a movable mirror [see Fig. 1(a)], with mass m, frequency ω, and damping rate γ. For our purposes, we can consider it to be a classical object whose deviation x_t from its equilibrium position ℓ_0 evolves through the equation [75,76]

$$m\ddot x_t + \gamma\dot x_t + m\omega^2 x_t = f_t. \tag{4}$$

Here, $f_t = \hbar G\langle a^\dagger a\rangle_t$, with $G = \omega_{\text{cav}}^0/\ell_0$, is the radiation-pressure force on the mirror in the linear-coupling regime, $|x_t|/\ell_0 \ll 1$, with $\omega_{\text{cav}} \approx \omega_{\text{cav}}^0(1 - x_t/\ell_0)$ [46,77].

This system can be interpreted as an engine [see Fig. 1(b)], or, more precisely, as an optomechanical energy converter. The atoms and light field represent the engine many-body *working fluid*. They absorb electromagnetic energy from the external driving and convert it into mechanical work which is delivered to the mirror to sustain its motion. The output power can be estimated as the heat dissipated by the mirror due to friction, thereby modeling a "dissipative load" [78].

III. NONEQUILIBRIUM THERMODYNAMICS

The mirror "state" (solely specified by instantaneous position x_t and velocity $\dot x_t$) and the state of the cavity-atom system ρ_t are in product form. Equation (3) provides the reduced quantum-system dynamics, parametrically depending on x_t via the cavity frequency ω_{cav}. Similarly, Eq. (4) provides the reduced mirror dynamics. This dynamical decoupling suggests that, also from a thermodynamic viewpoint, the cavity-atom system and the mirror can be regarded as uncorrelated. The mirror dynamics can be accounted for, e.g., within the framework of stochastic thermodynamics [76]. The challenge is, however, to consistently characterize the cavity-atom quantum engine.

The master equation [see Eq. (3)] is "local" [26] as it is obtained by a weak coupling of the system with a thermal bath [74] which, however, solely considers the bare-system Hamiltonians $H_{\text{at/cav}}$. This can be seen by the fact that $\mathcal{D}_{\text{at/cav}}$ do not implement transitions between eigenstates of the full Hamiltonian H but rather of $H_{\text{at/cav}}$. A thermodynamic approach considering as the internal energy the expectation of a total system Hamiltonian would thus run into inconsistencies [26,27,33] since it generically predicts negative entropy production for local master equations [79]. A textbook approach [1–6] considering the total Hamiltonian H and deriving a "global" master equation would not show any inconsistency. However, here, we are interested in providing a consistent description of the experimentally relevant [16,19] local master equation (3).

A. The first laws

Our approach takes inspiration from the separation, done in the framework of stochastic thermodynamics [75,76], between conservative forces [see the harmonic force in Eq. (4)] and nonconservative external ones [see the force f_t in Eq. (4)]. This entails the definition of two internal energies, one for the atoms and one for the light field, through the bare energies and the identification of the remainder of the Hamiltonian, e.g., the laser driving, as an external driving contribution.

We thus start by defining the atom internal energy as $u_t^{\mathrm{at}} := \langle H_{\mathrm{at}} \rangle_t$. Then, considering the generator $\mathcal{L}^*$, which is the dual of the generator $\mathcal{L}$ acting on observables, we find

$$\dot{u}_t^{\mathrm{at}} = \mathrm{Tr}(H_{\mathrm{at}} \mathcal{L}[\rho_t]) = \langle \mathcal{L}^*[H_{\mathrm{at}}] \rangle_t$$
$$= \frac{i}{\hbar} \langle [H, H_{\mathrm{at}}] \rangle_t + \langle \mathcal{D}_{\mathrm{at}}^*[H_{\mathrm{at}}] \rangle_t + \langle \mathcal{D}_{\mathrm{cav}}^*[H_{\mathrm{at}}] \rangle_t$$
$$= \frac{i}{\hbar} \langle [H_{\mathrm{las}}, H_{\mathrm{at}}] \rangle_t + \frac{i}{\hbar} \langle [H_{\mathrm{int}}, H_{\mathrm{at}}] \rangle_t + \langle \mathcal{D}_{\mathrm{at}}^*[H_{\mathrm{at}}] \rangle_t, \quad (5)$$

where the dissipators $\mathcal{D}_{\mathrm{at/cav}}^*$ are the dual dissipators for $\mathcal{D}_{\mathrm{at/cav}}$ in the Heisenberg picture. For the last equality, we used the fact that $\mathcal{D}_{\mathrm{cav}}^*$ acts nontrivially only on light-field operators. From the last line in Eq. (5), we can already identify the physical meaning of the different terms. The first term describes how the internal energy of the atoms varies due to the laser driving. The second describes the energy flows from the atoms to the light field, while the last term, which comes from the dissipator, describes the heat power exchanged by the atoms with their environment.

Instead of looking at the instantaneous currents, we want to take an average over a time window τ. The latter could be a period of the engine cycle or, in general, just a long time window. Time averaging Eq. (5), we find

$$\frac{1}{\tau} \int_0^\tau dt \, \dot{u}_t^{\mathrm{at}} = \frac{u_\tau^{\mathrm{at}} - u_0^{\mathrm{at}}}{\tau} = \mathcal{I}_{\mathrm{las}} - \mathcal{I}_{\mathrm{at}} - \mathcal{J}_{\mathrm{at}}. \quad (6)$$

Here, we have defined

$$\mathcal{I}_{\mathrm{las}} = \frac{i}{\hbar\tau} \int_0^\tau dt \, \langle [H_{\mathrm{las}}, H_{\mathrm{at}}] \rangle_t,$$
$$\mathcal{I}_{\mathrm{at}} = -\frac{i}{\hbar\tau} \int_0^\tau dt \, \langle [H_{\mathrm{int}}, H_{\mathrm{at}}] \rangle_t,$$
$$\mathcal{J}_{\mathrm{at}} = -\frac{1}{\tau} \int_0^\tau dt \, \langle \mathcal{D}_{\mathrm{at}}^*[H_{\mathrm{at}}] \rangle_t. \quad (7)$$

The term $\mathcal{I}_{\mathrm{las}}$ represents the time-averaged input power that the atoms receive from the laser, and the term $\mathcal{I}_{\mathrm{at}}$ is, instead, the average power exchanged between the atoms and the light field (in this convention it is positive when flowing from the atoms to the light field). The third term, $\mathcal{J}_{\mathrm{at}}$, is the average heat power dissipated by the atoms into the environment (this quantity is also positive when energy is leaving the atoms). Assuming that the integration time τ is large and the internal energy does not grow indefinitely with time, we have $\frac{u_\tau^{\mathrm{at}} - u_0^{\mathrm{at}}}{\tau} \to 0$, so from the above relation we can write

$$\mathcal{I}_{\mathrm{las}} = \mathcal{I}_{\mathrm{at}} + \mathcal{J}_{\mathrm{at}}. \quad (8)$$

The internal energy of the light field is defined as $u_t^{\mathrm{cav}} := \langle H_{\mathrm{cav}} \rangle_t$. By taking the time derivative and following a proce-

dure analogous to the one exploited in Eq. (5), we find

$$\dot{u}_t^{\mathrm{cav}} = \frac{i}{\hbar} \langle [H_{\mathrm{int}}, H_{\mathrm{cav}}] \rangle_t - f_t v_t + \langle \mathcal{D}_{\mathrm{cav}}^*[H_{\mathrm{cav}}] \rangle_t, \quad (9)$$

with $v_t := \dot{x}_t$ being the mirror velocity. Taking the time average over τ, the power absorbed by the light field due to the coupling with the atoms, $\mathcal{I}_{\mathrm{cav}} = i/(\hbar\tau) \int_0^\tau dt \, \langle [H_{\mathrm{int}}, H_{\mathrm{cav}}] \rangle_t$, is

$$\mathcal{I}_{\mathrm{cav}} = \mathcal{P}_{\mathrm{mir}} + \mathcal{J}_{\mathrm{cav}}, \quad (10)$$

where

$$\mathcal{P}_{\mathrm{mir}} = \frac{1}{\tau} \int_0^\tau dt \, f_t v_t, \quad \mathcal{J}_{\mathrm{cav}} = -\frac{1}{\tau} \int_0^\tau dt \, \langle \mathcal{D}_{\mathrm{cav}}^*[H_{\mathrm{cav}}] \rangle_t. \quad (11)$$

The first term above is the average heat power exchanged by the light field and the environment, while $\mathcal{P}_{\mathrm{mir}}$ is the power delivered by the cavity-atom system to the mirror. Exploiting the mirror internal energy $u_t^{\mathrm{mir}} = (mv_t^2 + m\omega^2 x_t^2)/2$ [75,76] and Eq. (4), we also find the relation

$$\mathcal{P}_{\mathrm{mir}} = \gamma/\tau \int_0^\tau dt \, v_t^2, \quad (12)$$

i.e., the power delivered by the cavity-atom system to the mirror is equal, over a long time window, to the power dissipated by the mirror due to friction [see Figs. 1(a) and 1(b)].

In order to find the total input power, we observe that the quantity $\mathcal{I}_{\mathrm{cav}} - \mathcal{I}_{\mathrm{at}}$ can be written as

$$\mathcal{I}_{\mathrm{cav}} - \mathcal{I}_{\mathrm{at}} = \frac{1}{\tau} \int_0^\tau dt \, \frac{i}{\hbar} \langle [H_{\mathrm{int}}, H_{\mathrm{at}} + H_{\mathrm{cav}}] \rangle_t.$$

This quantity can be different from zero whenever the atoms and the light field are not on resonance, in which case it represents an "imbalance" between the power delivered by the atoms and the power absorbed by the light field. We consider this imbalance, which comes from the interaction Hamiltonian and is due to energy gain or energy loss associated with the exchange of excitations, to be an additional input-power contribution. The rationale is that, in typical cavity-atom experiments, interactions between the atoms and the cavity field need to be "facilitated" by means of an additional laser driving, for instance, through stimulated Raman emissions [80]. In this sense, the imbalance term $\mathcal{I}_{\mathrm{cav}} - \mathcal{I}_{\mathrm{at}}$ is analogous, in spirit, to the term $\mathcal{I}_{\mathrm{las}}$. The total input is thus $\mathcal{I}_{\mathrm{in}} = \mathcal{I}_{\mathrm{las}} + \mathcal{I}_{\mathrm{cav}} - \mathcal{I}_{\mathrm{at}}$, which combining Eqs. (8)–(10), can be written as

$$\mathcal{I}_{\mathrm{in}} = \mathcal{J}_{\mathrm{cav}} + \mathcal{J}_{\mathrm{at}} + \mathcal{P}_{\mathrm{mir}}. \quad (13)$$

For the sake of simplicity, we have considered here a nonfluctuating mirror dynamics, which effectively accounts for a zero-temperature bath for the mirror. Similar results could be obtained for finite temperatures for the mirror. For the regimes investigated here, the power delivered by the engine would still be proportional to the square of the average mirror velocity (see, e.g., considerations in Ref. [59]).

B. The second law

In order to formulate a consistent efficiency for the optomechanical engine, we first need to show that the heat powers obey the inequality $\mathcal{J}_{\mathrm{at}} + \mathcal{J}_{\mathrm{cav}} \geqslant 0$. This is achieved by proving a suitable second law of thermodynamics through

a modification of Spohn's theorem [31,79,81]. To this end, we define the map $\mathcal{D} = \mathcal{D}_{\text{at}} + \mathcal{D}_{\text{cav}}$, whose stationary state is the thermal state $\rho^\beta \propto e^{-\beta(H_{\text{at}} + H_{\text{cav}})}$. Next, we consider the von Neumann entropy of the quantum state ρ_t, $S(\rho_t) = -\text{Tr}[\rho_t \ln \rho_t]$ and define the entropy production as

$$\sigma_t = \dot{S}(\rho_t) - \beta \text{Tr}\{\mathcal{D}[\rho_t](H_{\text{at}} + H_{\text{cav}})\}. \quad (14)$$

In the above equation, the first and second terms are the entropy and heat variations, respectively, and we further note that $\dot{S}(\rho_t) = -\text{Tr}\{\mathcal{D}[\rho_t] \ln \rho_t\}$. The task is now to show that the entropy production is always positive. We proceed by defining the relative entropy $S(\rho_t || \rho^\beta) = \text{Tr}[\rho_t(\ln \rho_t - \ln \rho^\beta)]$, which can only decrease under the action of a completely positive trace-preserving map [82]. Thus,

$$\frac{d}{du} S(e^{u\mathcal{D}}[\rho_t] || e^{u\mathcal{D}}[\rho^\beta])|_{u=0} \leqslant 0. \quad (15)$$

Since $e^{u\mathcal{D}}[\rho^\beta] = \rho^\beta$, the derivative of the relative entropy evaluated in $u = 0$ becomes

$$\frac{d}{du} S(e^{u\mathcal{D}}[\rho_t] || e^{u\mathcal{D}}[\rho^\beta])|_{u=0}$$
$$= -\dot{S}(\rho_t) + \beta \text{Tr}\{\mathcal{D}[\rho_t](H_{\text{at}} + H_{\text{cav}})\}. \quad (16)$$

The nonpositivity of the above quantity then implies the nonnegativity of the entropy production.

Averaging the entropy production over a long time window τ, we find

$$\frac{1}{\tau} \int_0^\tau dt\, \sigma_t = \frac{S(\rho_\tau) - S(\rho_0)}{\tau} + \beta(\mathcal{J}_{\text{at}} + \mathcal{J}_{\text{cav}}) \geqslant 0. \quad (17)$$

Now, assuming that $S(\rho_t)$ does not grow indefinitely with time, the above implies $\mathcal{J}_{\text{at}} + \mathcal{J}_{\text{cav}} \geqslant 0$, which is the inequality that we need. Before using this inequality to discuss the efficiency of the engine, we make an important remark on the above derivation. The main ingredient that we have exploited is that the reduced dynamics of the quantum state obeys the Lindblad equation (3), which only parametrically depends on the instantaneous position of the mirror x_t. The reduced dynamics of the quantum system assumes this form since the state of the mirror, fully specified by x_t and $\dot{x}_t$, and the quantum state are in product form. The product structure of the quantum-classical state also remains generically when considering single trajectories of stochastic dynamical equations for the mirror. However, when the mirror is promoted to a quantum degree of freedom, the derivation above requires appropriate modifications, given the emergence of intrinsic quantum correlations among all subsystems.

C. Efficiency

We are now able to obtain a thermodynamically consistent efficiency η of the energy conversion occurring in our optomechanical setup. The input power is equal, at long times, to the total power dissipated by the optomechanical system, i.e., $\mathcal{I}_{\text{in}} = \mathcal{P}_{\text{mir}} + \mathcal{J}_{\text{cav}} + \mathcal{J}_{\text{at}}$. Thus,

$$\eta = \frac{\mathcal{P}_{\text{mir}}}{\mathcal{P}_{\text{mir}} + \mathcal{J}_{\text{cav}} + \mathcal{J}_{\text{at}}} \leqslant 1. \quad (18)$$

The efficiency is bounded by 1 since both $\mathcal{P}_{\text{mir}}$ and $\mathcal{J}_{\text{at}} + \mathcal{J}_{\text{cav}}$ are positive, as shown in the previous section. Considering the total input power, Eq. (13), we can express $\mathcal{I}_{\text{in}}$ as in the denominator of Eq. (18) and identify a well-defined efficiency formulated in terms of the persistent heat currents.

IV. TIME-CRYSTAL ENGINE

As an application of the general theory that we have developed, we analyze power and efficiency for the recently introduced time-crystal engine [59].

For Markovian open quantum systems described by a time-independent Lindblad generator $\mathcal{L}$, one generically expects the density matrix of the system to converge for long times to a stationary state ρ_∞ such that $\mathcal{L}[\rho_\infty] = 0$. The generator $\mathcal{L}$ is time translation invariant due to its time independence and further commutes with the "time-translation operator" (propagator) $e^{t\mathcal{L}}$. Whenever the system approaches a steady state, one has $e^{t\mathcal{L}}[\rho_\infty] = \rho_\infty$, showing that ρ_∞ is *time translation symmetric* and thus obeys the same symmetry as the generator (see also, e.g., the discussion in Ref. [65]). The emergence of time-translation symmetry breaking, and thus of the so-called time-crystal phase, occurs when the state of the system approaches a limit cycle rather than a stationary state. By denoting with ρ_t^{lc} the state inside such an asymptotic limit cycle and assuming that the latter has period T, we find that $\rho_{t+T}^{\text{lc}} = \rho_t^{\text{lc}}$. In such a case, we have $e^{t'\mathcal{L}}[\rho_t^{\text{lc}}] = \rho_{t+t'}^{\text{lc}} \neq \rho_t^{\text{lc}}$ whenever $t, t' \neq T$. This shows that, despite the fact that the generator $\mathcal{L}$ is time translation symmetric, the asymptotic state of the system breaks such symmetry. In this case, the system features persistent oscillations and is said to enter a time-crystal phase. We note that signatures of the emergence of a time-crystal phase can be seen in the spectrum of the (finite-system) generator $\mathcal{L}$ [63].

We now proceed by discussing how time-translation symmetry breaking can be used as a power-generation mechanism in our setup [59]. In the regime in which the system approaches a stationary state, we find that the radiation-pressure force f_t becomes time independent for long times since it approaches its stationary value associated with the stationary state. In this case, the mirror is subject to a static force, and thus, its velocity converges to zero, leading to zero power production. On the other hand, in the time-crystal phase of the model, the state of the system features persistent oscillations so that the radiation-pressure force f_t remains asymptotically time dependent. As a consequence, the mirror is subject to a time-dependent force and thus never comes to rest and always sustains a finite velocity [16,19,63,80,83,84]. In the time-crystal regime, the mirror thus continuously dissipates power which must be provided by the time-crystal quantum engine. We note that, in the regime in which the Lindblad generator is time independent, the engine is clearly in contact with a single bath at fixed temperature. As such, the optomechanical engine in this setup does not function as a heat engine but rather as a nonequilibrium isothermal one [76].

A. Mean-field treatment

Since time-crystalline phases emerge only in the thermodynamic limit, we consider the system in the thermodynamic large-N limit, in which the quantum dynamics is exactly captured by a mean-field treatment [65]. That is, the rescaled
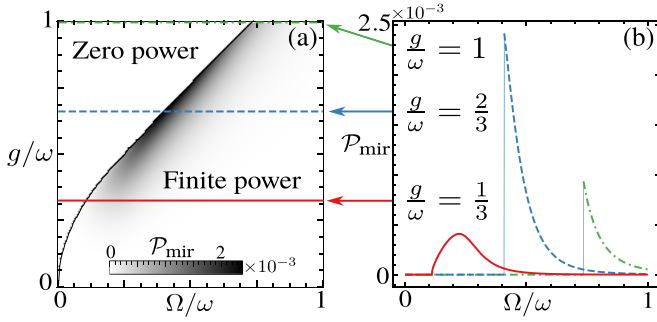
FIG. 2. Mechanical power output of the time-crystal quantum engine. (a) Power as a function of Ω and g, given in units of $\gamma(\Lambda\omega)^2$, with $\Lambda = \hbar GN/(m\omega^2)$. Note that, in our scaling limits, Λ remains finite for all N. The parameter γ is instead proportional to N in the infinite-density limit in which the optomechanical engine thus delivers extensive power output. The stationary phase (zero power) and the time-crystal phase (finite power) are separated by a critical line. (b) Three sections across (a) for different values of g. The solid line refers to $g/\omega = 1/3$, the dashed line refers to $g/\omega = 2/3$, and the dot-dashed line is associated with $g/\omega = 1$. The atoms are all initialized in the ground state and the light field in the vacuum. The parameters used are $\kappa = \gamma/m = \omega$.

operators $\alpha = a/\sqrt{N}$, $s_\pm = S_\pm/N$, and $s_z = S_z/N$, with $S_z = \sum_{k=1}^{N}(2n^{(k)} - 1)$, converge, with $N \to \infty$, to scalar quantities evolving through nonlinear equations [65,85,86]. For concreteness, we consider the case $\omega_{\text{at}} - \omega_{\text{cav}}^0 = \Delta = \nu = 0$ and $\beta \to \infty$, for which the equations are given by

$$\dot{s}_z = -2[i\Omega s_+ + ig\alpha s_+ + \text{c.c.}],$$

$$\dot{s}_+ = -i(\Omega + g\alpha^\dagger)s_z,$$

$$\dot{\alpha} = -\frac{\kappa}{2}\alpha + i[Gx\alpha - gs_-]. \tag{19}$$

As shown below (see also Figs. 2 and 3), for large Ω/g ratios the system state approaches indeed long-lived limit-cycle solutions [62,63,87]. In these cases, the radiation-pressure force is time dependent, and the mirror thus moves against friction, so that the cavity-atom engine delivers power [see $\mathcal{P}_{\text{mir}}$ in Eq. (11)] even without a time-dependent driving protocol [59]. In order to characterize the performance of the engine, we need to analyze the time evolution of the mirror and the dissipated power $\mathcal{P}_{\text{mir}}$ in the thermodynamic limit. However, the force f_t is extensive in N, $f_t \approx \hbar GN|\alpha_t|^2$, and this can give rise to an unphysical diverging displacement of the mirror. To arrive at a well-defined mirror dynamics [see Eq. (4)], in the thermodynamic limit, we identify below two suitable scaling regimes which are associated with two different physical scenarios.

B. Finite-density (weak-coupling) limit

First, we consider the regime in which, ideally, all atoms are located in the minima of an optical lattice inside the cavity [see sketch in Fig. 1(c)]. The cavity length is thus proportional to the number of atoms [16,59], i.e., $\ell_0 = N/D_0$, with D_0 being the linear density. The optomechanical coupling constant is here $G = \omega_{\text{cav}}^0 D_0/N$ and thus vanishes in the large-N limit. This scenario is associated with a weak optome-

chanical coupling [see Fig. 1(c)]. Looking at Eq. (19), this implies that the quantum-system dynamics does not depend on any of the mirror parameters. Still, the mirror dynamics is driven by the light-field intensity through the force $f_t = \hbar\omega_{\text{cav}}^0 D_0|\alpha_t|^2$, which, in this regime, becomes independent of N.

In Fig. 2(a), we show the power delivered by the engine to the mirror. We observe a parameter region in which the delivered power $\mathcal{P}_{\text{mir}}$ is zero. This occurs when the quantum system approaches a stationary state, the radiation-pressure force is a stationary value, and the mirror comes to rest, as is expected for static driving. Nonetheless, even with static driving, for certain parameters the quantum system can spontaneously enter a state of sustained oscillations, determining a time-dependent force on the mirror and thus a finite power $\mathcal{P}_{\text{mir}}$ [see Fig. 2(b)]. In this regime the optomechanical setup operates as a time-crystal quantum engine [59]. However, in the finite-density limit $\mathcal{P}_{\text{mir}}$ is intensive in N, while $\mathcal{J}_{\text{cav}} \propto N$, so that the engine efficiency is zero.

C. Infinite-density (strong-coupling) limit

We now introduce a regime in which the cavity-atom engine operates with finite efficiency. We consider the limit $N \to \infty$ while keeping ℓ_0 finite, which leads to an infinite density of atoms in the cavity [see the sketch in Fig. 1(c)] and to a finite G. We dub this limit the "strong" optomechanical coupling regime since the force f_t remains proportional to N. To have a physically meaningful mirror dynamics [see Eq. (4)], we rescale the mass and the friction parameter as $m = N\tilde{m}$ and $\gamma = N\tilde{\gamma}$, respectively. This means relating the size of the mirror to the number of atoms, which is natural when the "mirror" is a vibrational degree of freedom of the atom ensemble [11–13,20] or when the cavity hosts a cloud of atoms, as illustrated in Fig. 1(c). In this way, the mirror velocity remains finite, while the power is extensive in N, since $\gamma \propto N$. This gives the efficiency (at lowest order in Λ/ℓ_0)

$$\eta \approx \frac{\gamma}{\kappa m}\frac{\Lambda}{\ell_0}\frac{\int_0^{\omega\tau} d[\omega t]V_{\omega t}^2}{\int_0^{\omega\tau} d[\omega t]|\alpha_{\omega t}|^2}. \tag{20}$$

Here, $\Lambda = \hbar GN/(m\omega^2)$ is the characteristic length scale of x, while $V_{\omega t}$ is the dimensionless velocity at the dimensionless time ωt, such that $v_t = \Lambda\omega V_{\omega t}$. The complete expression of the efficiency, including finite temperature and finite atom decay, is given in Appendix A.

In this infinite-density limit, the dynamics of the quantum system is influenced by the motion of the mirror [see Eq. (19)]. For a timescale of the order of $(G\Lambda)^{-1}$, this back-action is irrelevant, and the cavity-atom system can host a (metastable) time-crystal phase [see Figs. 3(a) and 3(b) and Appendixes B and C]. Thereafter, back-action effects become non-negligible and drive the system towards a stationary state, where no power can be generated anymore.

Even if it appears as a metastable phase, we can characterize the time-crystal engine in the long prestationary regime. The average power is the same as that shown in Fig. 2, albeit now being extensive with N. The efficiency is reported in Figs. 3(c) and 3(d). It also signals the transition from the stationary to the (metastable) time-crystal phase, where the
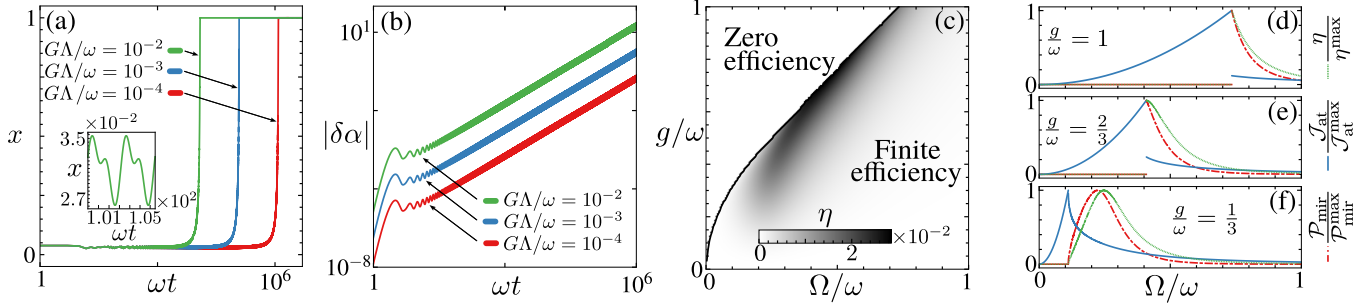
FIG. 3. Metastable time-crystal engine and efficiency in the infinite-density limit. (a) Mirror position x in units of Λ as a function of time for $\Omega = g = \omega$. The plot shows an emergent metastable regime in which the mirror features oscillations (see inset), unveiling that the quantum system is in a time-crystal phase. The smaller $G\Lambda/\omega$ (see arrows in the plot) is, the longer the metastable regime lasts before the system ends up in the stationary state. (b) Growth of the fluctuation $\delta\alpha$, associated with the light-field expectation α, due to the back-action of the dynamics of the mirror on the time evolution of the quantum system. The different lines refer to different values of $G\Lambda/\omega$, as indicated by the arrows in the plot. (c) Efficiency (in the metastable regime) in units of $\gamma\Lambda/(\kappa m \ell_0)$, obtained from Eq. (20). (d)–(f) Normalized power, light-field dissipation, and efficiency as a function of Ω for different values of g. The unspecified parameters are $\kappa = \gamma/m = \omega$.

system generates mechanical power. In Fig. 3(d), we see that for large g/ω the maximal power delivered by the engine occurs close to the transition line, where a maximal efficiency is also reached.

V. DISCUSSION

We characterized the nonequilibrium thermodynamics of phenomenological cavity-atom models. Contrary to other thermodynamic frameworks, our approach does not require the introduction of a repeated-interaction scheme [27–29]. It also does not consider as internal energy the expectation value of the total Hamiltonian [4,31,79]. We note that this is also what one would expected in the case of weak cavity-atom coupling, i.e., $\omega_{\text{at/cav}} \gg |\Omega|, |g|$. Instead, it relies on separating, within the system Hamiltonian, the bare-energy contributions from those related to external driving. This allows us to interpret dynamical contributions such as the laser driving as external power sources, which is closer, in spirit, to the physics of experiments with driven-dissipative quantum systems. Importantly, our identification of the different thermodynamic contributions leads to heat currents which are supported by the second law of thermodynamics. This leads to a well-defined energy-conversion efficiency. For concreteness, we illustrated our ideas considering a time-crystal engine [59]. However, our approach may also be applied more generally to cavity-only open quantum systems and to different manifestations of collective behavior hosted by them [12,60,88–93].

ACKNOWLEDGMENTS

APPENDIX A: DETAILS OF THE TWO THERMODYNAMIC LIMITS

We provide here details of the discussion reported in the main text concerning the two thermodynamic limits. We start deriving the quantities of interest, considering a finite number of atoms N. However, we already introduce the mean-field approximation since the latter becomes exact in the limit $N \to \infty$.

The time evolution of the relevant quantum operators is thus described by the mean-field equations reported in the main text. Through these operators we can write the heat currents as (derived for finite temperature)

$$\mathcal{J}_{\text{cav}} = \frac{\hbar\kappa}{\tau} \int_0^\tau dt \, \omega_{\text{cav}} \langle a^\dagger a - e^{-\beta\hbar\omega_{\text{cav}}}(1 + a^\dagger a)\rangle,$$

$$\mathcal{J}_{\text{at}} = \frac{\hbar\omega_{\text{at}}\nu}{\tau} \int_0^\tau dt \sum_{k=1}^N [(1 + e^{-\beta\hbar\omega_{\text{at}}})\langle n^{(k)}\rangle - e^{-\beta\hbar\omega_{\text{at}}}].$$
(A1)

To derive the mechanical output power, we need to look at the dynamics of the mirror, described by the second-order differential equation reported in the main text. The solution to this equation is given by $x_t = \Lambda X_{\omega t}$, with $\Lambda = \frac{\hbar G N}{m\omega^2}$ and

$$X_{\omega t} = \int_0^{\omega t} d[\omega s] \, |\alpha_{\omega s}|^2 e^{-\frac{\gamma_0}{\omega}(\omega t - \omega s)} \frac{\omega}{\Sigma} \sin\left[\frac{\Sigma}{\omega}(\omega t - \omega s)\right].$$
(A2)

Here, $\gamma_0 = \gamma/(2m)$, and we consider the dimensionless time ωt. Moreover, with a slight abuse of notation, we denote by $\alpha_{\omega t}$ the light-field operator at the dimensionless time ωt. Furthermore, by taking the derivative, we find the velocity of

the mirror as $v_t = \Lambda\omega V_{\omega t}$, with

$$V_{\omega t} = \int_0^{\omega t} d[\omega s]\, |\alpha_{\omega s}|^2 e^{-\frac{\gamma_0}{\omega}(\omega t - \omega s)}$$
$$\times \left(\cos\left[\frac{\Sigma}{\omega}(\omega t - \omega s)\right] - \frac{\gamma_0}{\Sigma}\sin\left[\frac{\Sigma}{\omega}(\omega t - \omega s)\right] \right). \tag{A3}$$

Here, $V_{\omega t}$ is the dimensionless velocity at the dimensionless time ωt. We note that $\dot{X}_{\omega t} = V_{\omega t}$ and $\dot{V}_{\omega t} = -X_{\omega t} - 2\gamma_0/\omega V_{\omega t} + |\alpha_{\omega t}|^2$, which is a dimensionless system of equations. Solving this combined with the mean-field equations, it is possible to compute the average mechanical output power as

$$\mathcal{P}_{\text{mirr}} = \frac{\gamma}{\tau}\int_0^\tau dt\, v_t^2 = \gamma(\Lambda\omega)^2 \left[\frac{1}{\omega\tau}\int_0^{\omega\tau} d[\omega t]V_{\omega t}^2\right].$$

1. Finite-density limit

We start by considering the finite-density limit. In this situation we have $G = \omega_{\text{cav}}^0 D_0/N$, which thus tends to zero in the large-N limit. This means that the mean-field equations become independent of x_t and that the quantum system does not feel the back-action due to the motion of the mirror.

In the finite-density limit, we find that $\Lambda = \hbar\omega_{\text{cav}}^0 D_0/(m\omega^2)$ and that the power $\mathcal{P}_{\text{mirr}}$ remains finite. However, as shown by Eqs. (A1), the heat fluxes are extensive with N, so the efficiency in this regime vanishes.

2. Infinite-density limit

In the infinite-density limit, the length of the cavity ℓ_0 remains independent of N. This means that G is finite in the thermodynamic limit. To have a well-defined dynamics for x_t we thus rescale the mass of the mirror, $m = N\tilde{m}$, as well as the friction parameter, $\gamma = N\tilde{\gamma}$. We note that Eqs. (A2) and (A3) remain valid and also that $\Lambda = \hbar G/(\tilde{m}\omega^2)$ does depend on N. The average mechanical power delivered by the optomechanical engine is now extensive since

$$\mathcal{P}_{\text{mirr}} = N\tilde{\gamma}(\Lambda\omega)^2 \left[\frac{1}{\omega\tau}\int_0^{\omega\tau} d[\omega t]V_{\omega t}^2\right].$$

The efficiency can be computed as

$$\eta = \frac{\mathcal{P}_{\text{mirr}}}{\mathcal{J}_{\text{cav}} + \mathcal{J}_{\text{at}} + \mathcal{P}_{\text{mirr}}} = \left(1 + \frac{\mathcal{J}_{\text{cav}} + \mathcal{J}_{\text{at}}}{\mathcal{P}_{\text{mirr}}}\right)^{-1},$$

and substituting for the relevant quantities, we find

$$\eta = \left(1 + \frac{\hbar\omega_{\text{at}}\nu}{\tilde{\gamma}(\Lambda\omega)^2} \frac{\int_0^{\omega\tau} d[\omega t][(1 + e^{-\beta\hbar\omega_{\text{at}}})n_{\omega t} - e^{-\beta\omega_{\text{at}}}]}{\int_0^{\omega\tau} d[\omega t]V_{\omega t}^2} \right.$$
$$\left. + \frac{\hbar\omega_{\text{cav}}^0\kappa}{\tilde{\gamma}(\Lambda\omega)^2} \frac{\int_0^{\omega\tau} d[\omega t](1 - \frac{\Lambda}{\ell_0}X_{\omega t})|\alpha_{\omega t}|^2(1 - e^{-\beta\hbar\omega_{\text{cav}}})}{\int_0^{\omega\tau} d[\omega t]V_{\omega t}^2}\right)^{-1}, \tag{A4}$$

where $n_{\omega t}$ is here the expectation value of the operator n at the dimensionless time ωt.

Specializing to the case with $\nu = 0$ and $\beta \to \infty$, we find, after manipulating the parameters, that

$$\eta \approx \frac{\gamma}{\kappa m}\frac{\Lambda}{\ell_0}\frac{\int_0^{\omega\tau} d[\omega t]V_{\omega t}^2}{\int_0^{\omega\tau} d[\omega t]|\alpha_{\omega t}|^2}, \tag{A5}$$

where we consider only the lowest order in Λ/ℓ_0.

APPENDIX B: METASTABLE TIME-CRYSTAL REGIME

We provide here details of the emergence of a metastable timescale where the optomechanical system works as a time-crystal engine with finite efficiency in the infinite-density limit. This timescale emerges when we consider the parameter $G\Lambda/\omega$ to be small, as we now show.

The evolution equation for $\alpha_{\omega t}$ is given by

$$\dot{\alpha}_{\omega t} = -\frac{\kappa}{2\omega}\alpha_{\omega t} + i\frac{G\Lambda}{\omega}\alpha_{\omega t} - i\frac{g}{\omega}s_{-\omega t}.$$

Considering $G\Lambda/\omega$ to be small, we can apply perturbation theory to the mean-field equations. By doing this, we can show that (see Appendix C for details)

$$\alpha_{\omega t} = \alpha_{\omega t}^0 + \frac{G\Lambda}{\omega}\delta\alpha_{\omega t}^1, \tag{B1}$$

where $\alpha_{\omega t}^0$ is obtained through the unperturbed system of mean-field equations, while the term $\delta\alpha_{\omega t}$ is the perturbation around this solution because we consider a small $G\Lambda/\omega$. In Fig. 3 in the main text, we provide the value $\delta\alpha = G\Lambda/\omega\delta\alpha^1$.

Now we proceed by rewriting the second-order differential equation for the mirror oscillations in terms of the dimensionless quantity $\epsilon = Gx/\omega$. We readily obtain

$$\ddot{\epsilon}_{\omega t} + \frac{\gamma}{m\omega}\dot{\epsilon}_{\omega t} + \epsilon_{\omega t} = \frac{G\Lambda}{\omega}|\alpha_{\omega t}|^2.$$

By recalling Eq. (B1), we see that up to first order in $G\Lambda/\omega$ the above equation is fully determined solely by the term $\alpha_{\omega t}^0$, which is given by the same system of equations solved for the finite-density limit and which can show persistent oscillations. However, the correction $\delta\alpha_{\omega t}$ increases linearly with time and thus eventually plays an important role in the dynamics of the mirror. Our exact numerical results show that the perturbation is such that the system will asymptotically approach a stationary state.

APPENDIX C: PERTURBATION THEORY ON THE MEAN-FIELD EQUATIONS

We give here a brief discussion of how we performed the perturbation theory to first order in $G\Lambda/\omega$.

In the dimensionless time, the mean-field equations become (we omit the explicit time dependence)

$$\dot{s}_z = -2\left[i\frac{\Omega}{\omega}s_+ + i\frac{g}{\omega}\alpha s_+ + \text{c.c.}\right],$$
$$\dot{s}_+ = -i\left(\frac{\Omega}{\omega} + \frac{g}{\omega}\alpha^\dagger\right)s_z,$$
$$\dot{\alpha} = -\frac{\kappa}{2\omega}\alpha + i\left[\frac{G\Lambda}{\omega}X\alpha - \frac{g}{\omega}s_-\right], \tag{C1}$$

where we used $x = \Lambda X$. This equation is coupled to the second-order differential [see discussion below Eq. (A3)]

$$\ddot{X} + 2\frac{\gamma_0}{\omega}\dot{X} + X = |\alpha|^2.$$

To zeroth order, we simply solve the above system by setting $G\Lambda/\omega \equiv 0$, which gives us the solutions s_z^0, s_+^0, and α^0.

To first order, we expect the solutions to be given by

$$s_z = s_z^0 + \frac{G\Lambda}{\omega}\delta s_z^1, \quad s_+ = s_+^0 + \frac{G\Lambda}{\omega}\delta s_+^1, \quad \alpha = \alpha^0 + \frac{G\Lambda}{\omega}\delta\alpha^1.$$

Substituting into the above system of equations, we find

$$\dot{\delta s_z^1} = -2\left[i\frac{\Omega}{\omega}\delta s_+^1 + i\frac{g}{\omega}(\alpha^0\delta s_+^1 + s_+^0\delta\alpha^1) + \text{c.c.}\right],$$

$$\dot{\delta s_+^1} = -i\frac{\Omega}{\omega}\delta s_z^1 - i\frac{g}{\omega}(\alpha^{0\dagger}\delta s_z^1 + s_z^0\delta\alpha^{1\dagger}),$$

$$\dot{\delta\alpha^1} = -\frac{\kappa}{2\omega}\delta\alpha^1 + iX^0\alpha^0 - i\frac{g}{\omega}\delta s_-^1. \tag{C2}$$

Solving these equations and combining them with the mean-field ones for the unperturbed variables s_z^0, s_+^0, and α^0 give the behavior of $\delta\alpha = (G\Lambda/\omega)\delta\alpha^1$ reported in the main text.

[1] R. Alicki, The quantum open system as a model of the heat engine, J. Phys. A **12**, L103 (1979).

[2] R. Kosloff, A quantum mechanical open system as a model of a heat engine, J. Chem. Phys. **80**, 1625 (1984).

[3] H. T. Quan, Y.-X. Liu, C. P. Sun, and F. Nori, Quantum thermodynamic cycles and quantum heat engines, Phys. Rev. E **76**, 031105 (2007).

[4] R. Kosloff, Quantum thermodynamics: A dynamical viewpoint, Entropy **15**, 2100 (2013).

[5] F. Binder, L. A. Correa, C. Gogolin, J. Anders, and G. Adesso, in *Thermodynamics in the Quantum Regime, Fundamental Aspects and New Directions*, 1st ed., edited by F. Binder, L. A. Correa, C. Gogolin, J. Anders, and G. Adesso, Fundamental Theories of Physics Vol. 195 (Springer, Cham, 2018), p. 998.

[6] S. Deffner and S. Campbell, *Quantum Thermodynamics: An Introduction to the Thermodynamics of Quantum Information* (Morgan and Claypool, San Rafael (USA), 2019).

[7] O. Abah, J. Roßnagel, G. Jacob, S. Deffner, F. Schmidt-Kaler, K. Singer, and E. Lutz, Single-Ion Heat Engine at Maximum Power, Phys. Rev. Lett. **109**, 203006 (2012).

[8] J. Roßnagel, S. T. Dawkins, K. N. Tolazzi, O. Abah, E. Lutz, F. Schmidt-Kaler, and K. Singer, A single-atom heat engine, Science **352**, 325 (2016).

[9] Q. Bouton, J. Nettersheim, S. Burgardt, D. Adam, E. Lutz, and A. Widera, A quantum heat engine driven by atomic collisions, Nat. Commun. **12**, 2063 (2021).

[10] F. Brennecke, T. Donner, S. Ritter, T. Bourdel, M. Köhl, and T. Esslinger, Cavity QED with a Bose–Einstein condensate, Nature (London) **450**, 268 (2007).

[11] F. Brennecke, S. Ritter, T. Donner, and T. Esslinger, Cavity optomechanics with a Bose-Einstein condensate, Science **322**, 235 (2008).

[12] K. W. Murch, K. L. Moore, S. Gupta, and D. M. Stamper-Kurn, Observation of quantum-measurement backaction with an ultracold atomic gas, Nat. Phys. **4**, 561 (2008).

[13] T. P. Purdy, D. W. C. Brooks, T. Botter, N. Brahms, Z.-Y. Ma, and D. M. Stamper-Kurn, Tunable Cavity Optomechanics with Ultracold Atoms, Phys. Rev. Lett. **105**, 133602 (2010).

[14] B. Chen, C. Jiang, J.-J. Li, and K.-D. Zhu, All-optical transistor based on a cavity optomechanical system with a Bose-Einstein condensate, Phys. Rev. A **84**, 055802 (2011).

[15] G. De Chiara, M. Paternostro, and G. M. Palma, Entanglement detection in hybrid optomechanical systems, Phys. Rev. A **83**, 052324 (2011).

[16] H. Ritsch, P. Domokos, F. Brennecke, and T. Esslinger, Cold atoms in cavity-generated dynamical optical potentials, Rev. Mod. Phys. **85**, 553 (2013).

[17] D. M. Stamper-Kurn, in *Cavity Optomechanics*, edited by M. Aspelmeyer, T. J. Kippenberg, and F. Marquardt (Springer, Heidelberg, 2014), Chap. 13, pp. 283–325.

[18] G. Labeyrie, E. Tesio, P. M. Gomes, G. L. Oppo, W. J. Firth, G. R. M. Robb, A. S. Arnold, R. Kaiser, and T. Ackemann, Optomechanical self-structuring in a cold atomic gas, Nat. Photonics **8**, 321 (2014).

[19] F. Mivehvar, F. Piazza, T. Donner, and H. Ritsch, Cavity QED with quantum gases: New paradigms in many-body physics, Adv. Phys. **70**, 1 (2021).

[20] H. Mikaeili, A. Dalafi, M. Ghanaatshoar, and B. Askari, Optomechanically induced gain using a trapped interacting Bose-Einstein condensate, Sci. Rep. **13**, 3659 (2023).

[21] C. Elouard and A. N. Jordan, Efficient Quantum Measurement Engines, Phys. Rev. Lett. **120**, 260601 (2018).

[22] W. Niedenzu, D. Gelbwaser-Klimovsky, A. G. Kofman, and G. Kurizki, On the operation of machines powered by quantum non-thermal baths, New J. Phys. **18**, 083012 (2016).

[23] T. Feldmann and R. Kosloff, Quantum four-stroke heat engine: Thermodynamic observables in a model with intrinsic friction, Phys. Rev. E **68**, 016101 (2003).

[24] Y. Rezek and R. Kosloff, Irreversible performance of a quantum harmonic heat engine, New J. Phys. **8**, 83 (2006).

[25] G. T. Landi and M. Paternostro, Irreversible entropy production: From classical to quantum, Rev. Mod. Phys. **93**, 035008 (2021).

[26] A. Levy and R. Kosloff, The local approach to quantum transport may violate the second law of thermodynamics, Europhys. Lett. **107**, 20004 (2014).

[27] F. Barra, The thermodynamic cost of driving quantum systems by their boundaries, Sci. Rep. **5**, 14873 (2015).

[28] P. Strasberg, G. Schaller, T. Brandes, and M. Esposito, Quantum and Information Thermodynamics: A Unifying Framework Based on Repeated Interactions, Phys. Rev. X **7**, 021003 (2017).

[29] G. D. Chiara, G. Landi, A. Hewgill, B. Reid, A. Ferraro, A. J. Roncaglia, and M. Antezza, Reconciliation of quantum local master equations with thermodynamics, New J. Phys. **20**, 113024 (2018).

[30] K. Micadei, J. P. Peterson, A. M. Souza, R. S. Sarthour, I. S. Oliveira, G. T. Landi, T. B. Batalhão, R. M. Serra, and E. Lutz, Reversing the direction of heat flow using quantum correlations, Nat. Commun. **10**, 2456 (2019).

[31] A. Hewgill, G. De Chiara, and A. Imparato, Quantum thermo-dynamically consistent local master equations, Phys. Rev. Res. **3**, 013165 (2021).

[32] W. Muschik, Phenomenological non-equilibrium quantum thermodynamics based on modified von Neumann equations, arXiv:2211.12558.

[33] J. T. Stockburger and T. Motz, Thermodynamic deficiencies of some simple Lindblad operators, Fortschr. Phys. **65**, 1600067 (2017).

[34] R. Dann and R. Kosloff, Quantum thermo-dynamical construction for driven open quantum systems, Quantum **5**, 590 (2021).

[35] N. Defenu, T. Donner, T. Macrì, G. Pagano, S. Ruffo, and A. Trombettoni, Long-range interacting quantum systems, arXiv:2109.01063.

[36] A. P. Solon, Y. Fily, A. Baskaran, M. E. Cates, Y. Kafri, M. Kardar, and J. Tailleur, Pressure is not a state function for generic active fluids, Nat. Phys. **11**, 673 (2015).

[37] A. P. Solon, J. Stenhammar, M. E. Cates, Y. Kafri, and J. Tailleur, Generalized thermodynamics of phase equilibria in scalar active matter, Phys. Rev. E **97**, 020602(R) (2018).

[38] A. P. Solon, J. Stenhammar, M. E. Cates, Y. Kafri, and J. Tailleur, Generalized thermodynamics of motility-induced phase separation: Phase equilibria, Laplace pressure, and change of ensembles, New J. Phys. **20**, 075001 (2018).

[39] É. Fodor, R. L. Jack, and M. E. Cates, Irreversibility and biased ensembles in active matter: Insights from stochastic thermodynamics, Annu. Rev. Condens. Matter Phys. **13**, 215 (2022).

[40] É. Fodor and M. E. Cates, Active engines: Thermodynamics moves forward, Europhys. Lett. **134**, 10003 (2021).

[41] C. Nardini, E. Fodor, E. Tjhung, F. van Wijland, J. Tailleur, and M. E. Cates, Entropy Production in Field Theories without Time-Reversal Symmetry: Quantifying the Non-Equilibrium Character of Active Matter, Phys. Rev. X **7**, 021007 (2017).

[42] E. Fodor, C. Nardini, M. E. Cates, J. Tailleur, P. Visco, and F. van Wijland, How Far from Equilibrium Is Active Matter? Phys. Rev. Lett. **117**, 038103 (2016).

[43] A. Riera, C. Gogolin, and J. Eisert, Thermalization in Nature and on a Quantum Computer, Phys. Rev. Lett. **108**, 080402 (2012).

[44] T. J. Kippenberg, H. Rokhsari, T. Carmon, A. Scherer, and K. J. Vahala, Analysis of Radiation-Pressure Induced Mechanical Oscillation of an Optical Microcavity, Phys. Rev. Lett. **95**, 033901 (2005).

[45] A. Jayich, J. Sankey, B. Zwickl, C. Yang, J. Thompson, S. Girvin, A. Clerk, F. Marquardt, and J. Harris, Dispersive optomechanics: A membrane inside a cavity, New J. Phys. **10**, 095008 (2008).

[46] M. Aspelmeyer, T. J. Kippenberg, and F. Marquardt, Cavity optomechanics, Rev. Mod. Phys. **86**, 1391 (2014).

[47] V. Dumont, H.-K. Lau, A. A. Clerk, and J. C. Sankey, Asymmetry-Based Quantum Backaction Suppression in Quadratic Optomechanics, Phys. Rev. Lett. **129**, 063604 (2022).

[48] M. Lei, R. Fukumori, J. Rochman, B. Zhu, M. Endres, J. Choi, and A. Faraon, Many-body cavity quantum electrodynamics with driven inhomogeneous emitters, Nature **617**, 271 (2023).

[49] K. Zhang, F. Bariani, and P. Meystre, Quantum Optomechanical Heat Engine, Phys. Rev. Lett. **112**, 150602 (2014).

[50] K. Zhang, F. Bariani, and P. Meystre, Theory of an optomechanical quantum heat engine, Phys. Rev. A **90**, 023819 (2014).

[51] C. Elouard, M. Richard, and A. Auffèves, Reversible work extraction in a hybrid opto-mechanical system, New J. Phys. **17**, 055018 (2015).

[52] D. Gelbwaser-Klimovsky and G. Kurizki, Work extraction from heat-powered quantized optomechanical setups, Sci. Rep. **5**, 7809 (2015).

[53] A. Mari, A. Farace, and V. Giovannetti, Quantum optomechanical piston engines powered by heat, J. Phys. B **48**, 175501 (2015).

[54] M. Brunelli, A. Xuereb, A. Ferraro, G. D. Chiara, N. Kiesel, and M. Paternostro, Out-of-equilibrium thermodynamics of quantum optomechanical systems, New J. Phys. **17**, 035016 (2015).

[55] F. Reif, *Fundamentals of Statistical and Thermal Physics* (Waveland, Long Grove (USA), 2009).

[56] F. Minganti, A. Biella, N. Bartolo, and C. Ciuti, Spectral theory of Liouvillians for dissipative phase transitions, Phys. Rev. A **98**, 042118 (2018).

[57] W. Casteels, R. Fazio, and C. Ciuti, Critical dynamical properties of a first-order dissipative phase transition, Phys. Rev. A **95**, 012128 (2017).

[58] H. J. Carmichael, Breakdown of Photon Blockade: A Dissipative Quantum Phase Transition in Zero Dimensions, Phys. Rev. X **5**, 031028 (2015).

[59] F. Carollo, K. Brandner, and I. Lesanovsky, Nonequilibrium Many-Body Quantum Engine Driven by Time-Translation Symmetry Breaking, Phys. Rev. Lett. **125**, 240602 (2020).

[60] F. Bibak, U. Delić, M. Aspelmeyer, and B. Dakić, Dissipative phase transitions in optomechanical systems, J. Phys. A **107**, 053505 (2023).

[61] F. Wilczek, Quantum Time Crystals, Phys. Rev. Lett. **109**, 160401 (2012).

[62] B. Buča, J. Tindall, and D. Jaksch, Non-stationary coherent quantum many-body dynamics through dissipation, Nat. Commun. **10**, 1730 (2019).

[63] F. Iemini, A. Russomanno, J. Keeling, M. Schirò, M. Dalmonte, and R. Fazio, Boundary Time Crystals, Phys. Rev. Lett. **121**, 035301 (2018).

[64] K. Sacha and J. Zakrzewski, Time crystals: A review, Rep. Prog. Phys. **81**, 016401 (2018).

[65] F. Carollo and I. Lesanovsky, Exactness of Mean-Field Equations for Open Dicke Models with an Application to Pattern Retrieval Dynamics, Phys. Rev. Lett. **126**, 230601 (2021).

[66] P. Bruno, Impossibility of Spontaneously Rotating Time Crystals: A No-Go Theorem, Phys. Rev. Lett. **111**, 070402 (2013).

[67] H. Watanabe and M. Oshikawa, Absence of Quantum Time Crystals, Phys. Rev. Lett. **114**, 251603 (2015).

[68] F. M. Gambetta, W. Li, F. Schmidt-Kaler, and I. Lesanovsky, Engineering Nonbinary Rydberg Interactions via Phonons in an Optical Lattice, Phys. Rev. Lett. **124**, 043402 (2020).

[69] F. Carollo, F. M. Gambetta, K. Brandner, J. P. Garrahan, and I. Lesanovsky, Nonequilibrium Quantum Many-Body Rydberg Atom Engine, Phys. Rev. Lett. **124**, 170602 (2020).

[70] A. Blais, A. L. Grimsmo, S. M. Girvin, and A. Wallraff, Circuit quantum electrodynamics, Rev. Mod. Phys. **93**, 025005 (2021).

[71] E. T. Jaynes and F. W. Cummings, Comparison of quantum and semiclassical radiation theories with application to the beam maser, Proc. IEEE **51**, 89 (1963).

[72] K. Hepp and E. H. Lieb, On the superradiant phase transition for molecules in a quantized radiation field: The Dicke maser model, Ann. Phys. (NY) **76**, 360 (1973).

[73] K. Hepp and E. H. Lieb, Equilibrium statistical mechanics of matter interacting with the quantized radiation field, Phys. Rev. A **8**, 2517 (1973).

[74] H.-P. Breuer and F. Petruccione, *The Theory of Open Quantum Systems* (Oxford University Press, Oxford, 2002).

[75] T. Tomé and M. J. De Oliveira, *Stochastic Dynamics and Irreversibility* (Springer, New York (USA), 2015).

[76] U. Seifert, Stochastic thermodynamics, fluctuation theorems and molecular machines, Rep. Prog. Phys. **75**, 126001 (2012).

[77] F. Marquardt, J. G. E. Harris, and S. M. Girvin, Dynamical Multistability Induced by Radiation Pressure in High-Finesse Micromechanical Optical Cavities, Phys. Rev. Lett. **96**, 103901 (2006).

[78] S. Seah, S. Nimmrichter, and V. Scarani, Work production of quantum rotor engines, New J. Phys. **20**, 043045 (2018).

[79] K. Brandner and U. Seifert, Periodic thermodynamics of open quantum systems, Phys. Rev. E **93**, 062134 (2016).

[80] P. Kirton, M. M. Roses, J. Keeling, and E. G. Dalla Torre, Introduction to the Dicke Model: From Equilibrium to Nonequilibrium, and Vice Versa, Adv. Quantum Technol. **2**, 1800043 (2019).

[81] H. Spohn, Entropy production for quantum dynamical semigroups, J. Math. Phys. **19**, 1227 (1978).

[82] V. Vedral, The role of relative entropy in quantum information theory, Rev. Mod. Phys. **74**, 197 (2002).

[83] A. Tomadin and R. Fazio, Many-body phenomena in QED-cavity arrays, J. Opt. Soc. Am. B **27**, A130 (2010).

[84] F. Piazza and H. Ritsch, Self-Ordered Limit Cycles, Chaos, and Phase Slippage with a Superfluid inside an Optical Resonator, Phys. Rev. Lett. **115**, 163601 (2015).

[85] F. Benatti, F. Carollo, R. Floreanini, and H. Narnhofer, Non-Markovian mesoscopic dissipative dynamics of open quantum spin chains, Phys. Lett. A **380**, 381 (2016).

[86] F. Benatti, F. Carollo, R. Floreanini, and H. Narnhofer, Quantum spin chain dissipative mean-field dynamics, J. Phys. A **51**, 325001 (2018).

[87] F. Carollo and I. Lesanovsky, Exact solution of a boundary time-crystal phase transition: Time-translation symmetry breaking and non-Markovian dynamics of correlations, Phys. Rev. A **105**, L040202 (2022).

[88] E. Verhagen, S. Deléglise, S. Weis, A. Schliesser, and T. J. Kippenberg, Quantum-coherent coupling of a mechanical oscillator to an optical cavity mode, Nature (London) **482**, 63 (2012).

[89] M. Maldovan and E. L. Thomas, Simultaneous localization of photons and phonons in two-dimensional periodic structures, Appl. Phys. Lett. **88**, 251907 (2006).

[90] M. Eichenfield, R. Camacho, J. Chan, K. J. Vahala, and O. Painter, A picogram- and nanometre-scale photonic-crystal optomechanical cavity, Nature (London) **459**, 550 (2009).

[91] P. Bertet, S. Osnaghi, P. Milman, A. Auffeves, P. Maioli, M. Brune, J. M. Raimond, and S. Haroche, Generating and Probing a Two-Photon Fock State with a Single Atom in a Cavity, Phys. Rev. Lett. **88**, 143601 (2002).

[92] A. Frisk Kockum, A. Miranowicz, S. De Liberato, S. Savasta, and F. Nori, Ultrastrong coupling between light and matter, Nat. Rev. Phys. **1**, 19 (2019).

[93] A. Camacho-Guardian and N. R. Cooper, Moiré-Induced Optical Nonlinearities: Single- and Multiphoton Resonances, Phys. Rev. Lett. **128**, 207401 (2022).